STYLES OF EJECTA EMPLACEMENT, METEOR CRATER; P.H. Schultz and J.A. Grant, Dept. Geological Sciences, Brown University, Providence, RI 02912.

Laboratory impact experiments at the NASA–Ames Vertical Gun Range (AVGR) provide a unique look at impact ejecta dynamics and emplacement in the presence of an atmosphere (1, 2). Although rigid scaling criteria cannot be met simultaneously, such experiments provide an invaluable perspective for certain processes or trends that should generally apply at broader scales. As a first step to test these insights, a preliminary analysis of ejecta size distributions and gross ejecta blanket morphology at Meteor Crater has been undertaken. We first review the laboratory results and then examine possible applications to field studies at Meteor Crater.

Review of Laboratory Results: Five ejecta emplacement styles characterize impacts under atmospheric conditions. First, vaporization of target materials has been observed to produce a rapidly expanding blast that scours the surface out to 10 crater radii from the rim (3). This precursor *Scour Phase* is best developed for impacts at angles less than 30° when the released gases are decoupled from the crater cavity. Analytical solutions (and observations in the laboratory) indicate that this vapor–induced scouring phase is short lived, and atmospheric conditions return to near ambient levels prior to ejecta emplacement. Resultant features include a broad scouring of the pre–impact surface found below the ejecta deposits and extending to large distances from the impact.

Second, ejecta exceeding a critical size (dependent on crater scale for a given atmospheric pressure and gravity) are aerodynamically separated from smaller ejecta and advance outward in a widening funnel–shaped cone typical of impacts under vacuum conditions. This stage of *Aerodynamic Sorting* is observed in the laboratory (2) as well as in much broader scale explosions (4).

Third, for atmospheric pressures within a certain range (0.05–0.25 P_o), laboratory experiments indicate a stage of *Wind–Driven Vortical Flow.* The "wind" is mechanically driven by the advancing curtain and entrains finer ejecta fractions. The outward–moving circulation of ejecta and air can suspend much larger ballistically transported ejecta until the pressure differential in front of and behind the curtain reduces below a critical level. Large ejecta entrained in this circulation can come from nearly all excavated horizons and are eventually deposited to form a ridge or rampart once the wind–driving force disappears. Figure 1 illustrates the concentration of coarser fragments within the rampart of a laboratory crater. The maximum diameter of the rampart depends on the degree of entrainment: it increases with increasing atmospheric density, increasing wind velocity (curtain velocity, i.e., scale) and decreasing ejecta size. Scaling considerations (2) indicate that this emplacement style is possible for craters 0.5–5 km in diameter on the Earth and 1.5–15 km on Mars if a significant fraction (10%) of the ejecta is smaller than 0.5 cm.

Fourth, *Fluidized Ejecta Flow* develops in laboratory craters for sufficiently high atmospheric pressures (0.3–0.8 P_o) and sufficiently small ejecta sizes (<100 μ). Individual flow lobes with rampart–bordered fronts have been observed to run–up relief and extend up to 6 crater–radii from the rim. Ejecta dominated by finer fractions favor this emplacement style. In the laboratory, bimodal size distributions enhance the development of simple ejecta ramparts at the expense of fluidized flow. Fluidized ejecta flow result in fine–size ejecta being transported well beyond the range expected for ballistic transport subject to air drag. Extremely fine ejecta and/or very high atmospheric densities result in a much more turbulent emplacement style characterized by radial scouring of the inner ejecta facies and fall–out in the outer facies.

Fifth, collapse of a thermally lofted cloud of non–ballistic ejecta is observed in explosion craters but not in the laboratory experiments. The occurrence of this *Gravity–Driven Cloud Collapse* is suspected on the basis of recent studies of the suevite at the Ries Crater, Germany (5) and late–stage radial scouring of certain multi–lobed martian craters (6). Deposits from such a process should be dominated by the deepest pre–impact horizons reflecting separation from the earlier stages of mechanically driven (shock–induced) flow of the target.

Meteor Crater: Ambient terrestrial atmospheric pressure and the size distribution of grains comprising the pre–impact limestone and sandstone stratigraphy at Meteor Crater would be expected to result in a fluidized–ejecta emplacement style for a 1 km–diameter crater. Because this size crater is close to onset of strength–controlled crater growth, however, large ejecta fragments should be expected to produce a bimodal size distribution, thereby favoring the development of a rampart of coarse debris analogous to the laboratory results. With this perspective, a preliminary field study of the ejecta emplacment style and ejecta size distributions was performed. Four of the five ejecta emplacement styles listed above can be recognized: ballistic emplacement of blocks at large distances, behind pre–impact topographic barriers, and on top the ejecta (late–stage high–angle debris); fluidized ejecta flow; a relatively well preserved ejecta rampart encircling portions of the crater; and highly localized late-stage emplacement of hydrothermally altered, deep-seated ejecta near the crater rim. Evidence for pre-impact scouring appears to have been largely removed by subsequent erosion. A separate contribution (7) presents a closer look at the overall erosional state of the ejecta.

A pre-impact ridge of Moenkopi silt/sandstone ~2 crater radii northwest of the crater provides important clues for distinguishing ballistic and possibly non-ballistic emplacement styles. Uprange, ejecta deposits are poorly sorted with a significant fine-grained component. A distinctive lobe of finely powdered ejecta mixed with fragments from the Moenkopi, Kaibab, and Coconino formations extends up and onto the ridge. Surface expression of the deposit is partly masked by a 3–4 cm thick reddish-stained lag. Downrange at the ridge base, ejecta deposits are notably absent but reappear at greater distances as numerous blocks within a matrix of fragmental debris notably coarser than the deposits on and uprange from the ridge. Only along a breach in the ridge does the finer ejecta deposit extend downrange. We suggest that the Moenkopi ridge acted as a barrier for a ground-hugging debris-entrained ejecta flow and created a ballistic shadow for coarser debris downrange.

Additional evidence for ballistically emplaced blocks was found on the ejecta about 0.5 R from the crater rim. Several blocks ranging from ~1 to 3 m across each were found in shallow, rimmed depressions characteristicaly surrounded by fragments, which are often more abundant downrange. These blocks are typically radial to points where the crater rim is unusually low. Because they occur on top of the ejecta, they must have been late arriving, perhaps due to high-angle trajectories created during formation of the breach in the rim.

Stereo-photography, topographic profiles, and drainage patterns clearly reveal a 5–15 m ridge best developed about 0.5R–0.8R southwest, south, and southeast of the crater. Shoemaker (8) interpreted this plateau as a Pleistocene pediment, but other evidence for relatively little erosion of the ejecta (7) suggests that this feature is a preserved primary structure. Analysis of the ejecta size distributions below the weathering horizon reveals that sizes smaller than 1.5 cm (–4.0θ) typically are bimodal, and preliminary observations in exposed outcrops indicate that large (0.5m – 1 m) blocks from all stratigraphic horizons further add to the bimodal character of the deposit. These observations are consistent with the interpretation that the ridge marks the terminal boundary of a clastic debris flow perhaps analogous to the wind-driven vortical flow observed in the laboratory.

Finally, an unusual 1–2 m near-surface layer of hydrothermally modified Coconino was found on the rim. The outcrop is characterized by numerous long (1–5 cm), hollow, iron-stained tubes, (degassing pipes ?), and vesicular and frothy-like welded Coconino. Kieffer (8) interpreted similar occurrences within the crater as interactions between silica melt and water vapor. This unit may be analogous to the gas-charged suevite at the Ries Crater (5), Germany, perhaps representing late-stage collapse of a hot, gas-charged cloud that formed an ignimbrite-like flow. This is the only clear evidence that we found for possible water-impact interactions beyond the crater rim.

Summary: We recognize that our observations and interpretations are contrary to previous studies. Nevertheless, Meteor Crater allows a unique view of the complexities in ejecta emplacement that may require a new view in the context of physical models. One such context is the consequences of dynamic interactions with the atmosphere as observed at much smaller laboratory scales. Further studies should provide better constraints and tests for such applications, including limits on the role of unbound water on the emplacement process.

(1) Schultz P.H. and Gault D.E (1979) *J. Geophys. Res.*, *84*, pp. 7669–7687 (2) Schultz P.H. (1986) *MECA Symposium on Mars: Evolution of its Climate and Atmosphere* (abstract), pp. 95–97, Lunar and Planetary Institute, Houston. (3) Schultz P.H (1988) *Lunar and Planet. Sci. XIX*, pp. 1039–1040, Lunar and Planetary Institute, Houston. (4) Wisotski J. (1977) In *Impact and Explosion Cratering* (D. Roddy *et al.*, eds.), pp. 1101–1121, Pergamon, New York (5) Newsom H. *et al.* (1988) preprint. (6) Schultz P.H. and Singer J. (1980) *Proc. Lunar Planet. Sci. XI*, pp. 2243–2259, Lunar and Planetary Institute, Houston. (7) Grant J. and Schultz P H (1989) *Lunar and Planet Sci. XX* (this volume). (8) Shoemaker E.M. and Kieffer S.E. (1974) *Guidebook to the Geology of Meteor Crater, Arizona*. ASU Center for Meteorite Studies Pub. *17*, Tempe, AZ, 66 p.

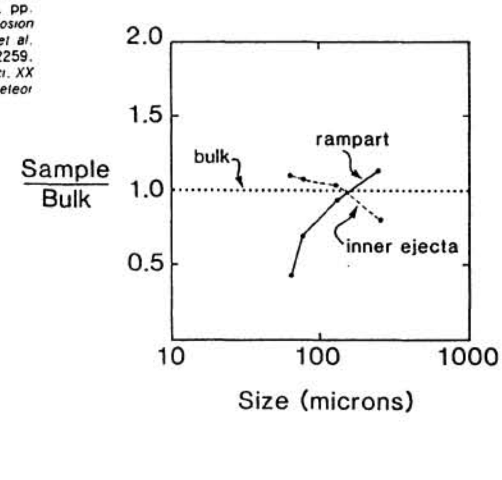

Figure 1. Entrainment and deposition of larger size fractions in the contiguous rampart of laboratory craters.